Active colloidal suspensions: Clustering and phase behavior

Julian Bialké [a,*], Thomas Speck [b], Hartmut Löwen [a]

[a] Institut für Theoretische Physik II, Heinrich-Heine-Universität, D-40225 Düsseldorf, Germany
[b] Institut für Physik, Johannes Gutenberg-Universität Mainz, Staudingerweg 7-9, D-55128 Mainz, Germany

ABSTRACT

We review recent experimental, numerical, and analytical results on active suspensions of self-propelled colloidal beads moving in (quasi-)two dimensions. Active colloids form part of the larger theme of *active matter*, which is noted for the emergence of collective dynamic phenomena away from thermal equilibrium. Both in experiments and computer simulations, a separation into dense aggregates, i.e., clusters, and a dilute gas phase has been reported even when attractive interactions and an alignment mechanism are absent. Here, we describe three experimental setups, discuss the different propelling mechanisms, and summarize the evidence for phase separation. We then compare experimental observations with numerical studies based on a minimal model of colloidal swimmers. Finally, we review a mean-field approach derived from first principles, which provides a theoretical framework for the density instability causing the phase separation in active colloids.

© 2014 Elsevier B.V. All rights reserved.

1. Introduction

In the past decade, active systems have gained enormous interest in the field of soft matter physics from both the experimental and the theoretical side, see Refs. [1–4] for recent general reviews. Motivated through not only macroscopic biological systems like flock of birds [5] and school of fish [6], but also microscopic systems like bacterial colonies [7,8], theoretical models of self-propelled particles have been developed that demonstrate the emergence of collective phenomena from simple idealized interactions [9,10]. Theoretical descriptions have mainly focused on hydrodynamic approaches describing the coarse-grained dynamics on large scales [11]. Coefficients are either treated as free parameters or are derived, e.g., from the microscopic modeling of collisions [12–14]. In these models, the crucial interaction mechanism responsible for collective behavior such as laning, swarming, and even active turbulence [15–17] is the alignment of velocities, or orientations. These interactions might be cognitive as in the case of birds, or physical due to, e.g., volume exclusion of granular rods [18] and disks [19].

More recently, experimental setups of artificial colloidal "swimmers" have been realized, the propulsion properties of which can be tuned. Directed phoretic motion of these colloidal particles is the hydrodynamic consequence of maintaining a local gradient of a molecular solvent, e.g. due to chemical reactions on the different surface areas of a particle in a hydrogen peroxide mixture [20–22], or the local demixing of a water–lutidine mixture at one side of the particle [23]. Moderately dense *active suspensions* of such artificial swimmers can be realized and studied [24,

25], for a summary of the experiments see Fig. 1. Arguably the most interesting feature is that a clustering of particles is observed. These clusters are very dynamic, and particles join and leave as shown in Fig. 1(b). While the cluster size in these experiments seems to reach saturation, in another experiment [26] using the reversible demixing of a binary solvent evidence for phase separation into compact large clusters and a dilute gas phase of free swimmers has been presented.

Such a phase separation has also been observed in computer simulations of a minimal model [26–33]. In this model, disks are propelled with constant velocity along their orientations, which undergo free rotational diffusion. Moreover, disks interact via a purely repulsive pair potential. The existence of a collective phase transition is somewhat surprising given that this model lacks both attractions – leading to phase separation in passive suspensions – and an alignment mechanism. Still, the persistence of the directed motion in combination with volume exclusion forces leads to a self-trapping phenomenon, where particles get temporally "stuck" and block each other, which has also been shown for lattice models before [34,35]. Tailleur and Cates have shown theoretically for a model of run-and-tumble bacteria that indeed a locally reduced mobility is sufficient to give rise to a separation into dense *slow* regions, where directed motion is blocked, and a dilute gas of fast particles [36–38].

Instead of giving a general overview, in this article we focus on recent experimental and theoretical progress on the phase behavior of self-propelled colloidal particles in two dimensions without an alignment mechanism. First, we review results from three groundbreaking experimental setups that have realized (quasi-)two-dimensional systems of spherical swimmers with a controllable propelling speed v_0 of the order μm/s, where the correlation between the particle orientations, i.e., the direction of propulsion, appears to be negligible, see
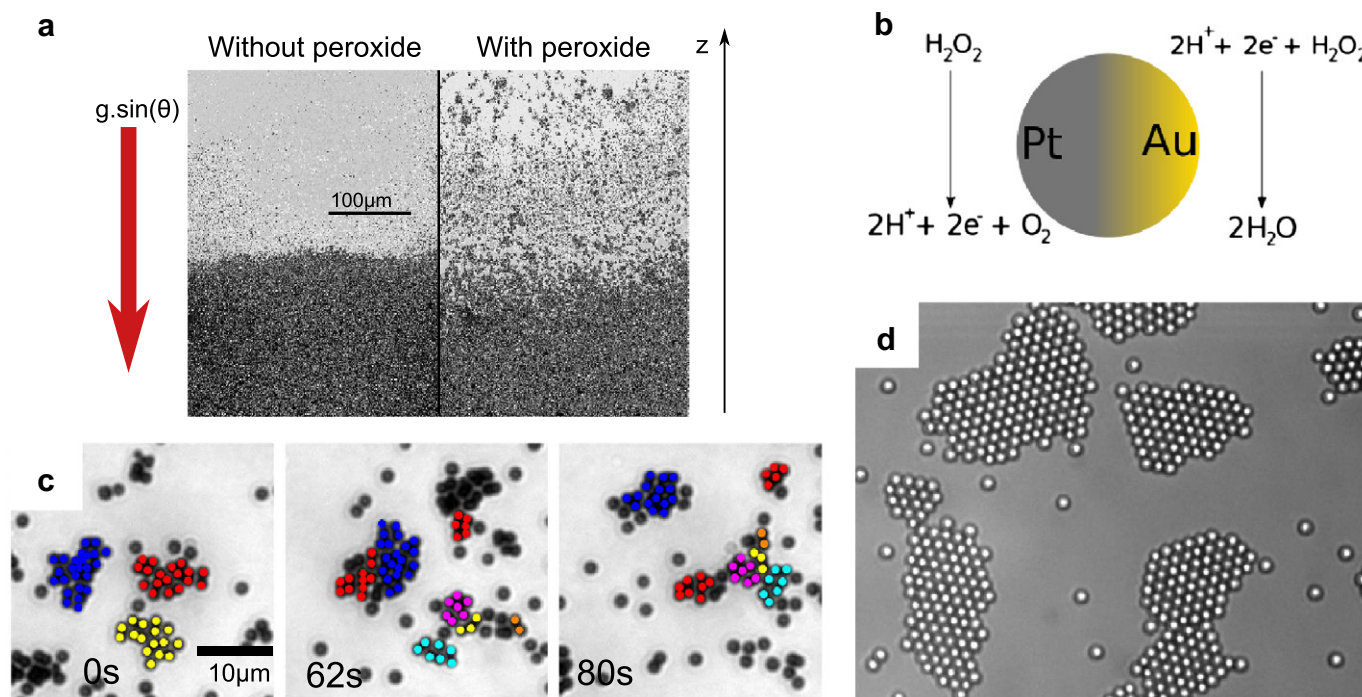
Fig. 1. Suspensions of catalytic Janus particles close to a surface: (a) Snapshots of platinum coated gold particles without (left) and with "fuel" (right) in the experiments of Theurkauff et al. [24]. Particles have sunk to the bottom of a tilted cell, where they accumulate at the bottom. In the active suspension (right), a smeared interface between a dense phase at the bottom and a dilute gas phase at the top is observed. (b) Cluster formation in the dilute phase in the experiment of Theurkauff et al. Colors indicate membership of a cluster at $t = 0$ and demonstrate how clusters evolve. (c) The platinum acts as a catalyst for the decomposition of hydrogen peroxide. The actual swimming mechanism is still somewhat debated, see text. (d) Formation of large clusters, "living crystals", in a related experiment performed by Palacci et al. [25] using colloidal particles with an embedded hematite cube. The catalytic activity of the hematite is controlled externally through light.
Figure adapted from Refs. [24,25].

Supplementary Material of Ref. [26]. A minimal model is then described, which nevertheless captures the relevant ingredients of the experiments. We discuss numerical results based on this model and compare them to experimental results. We briefly discuss the influence of hydrodynamic interactions as well as freezing of active systems at high densities. Finally, we introduce a mean-field approach leading to evolution equations for the density and the orientational field of an active suspension [30]. The crucial role in this theory is played by a single parameter, the force imbalance due to an anisotropic pair distribution. We then conclude and outline possible directions for further research in this rapidly evolving field.

2. Experimental evidence

2.1. Clustering of catalytic swimmers

For colloidal particles to "swim" autonomously, at least the following two conditions need to be met: (i) besides the colloidal solute and the solvent, there is a molecular solute and (ii) the distribution of this molecular solute is kept asymmetric.[1] Two practical schemes have been realized for the study of (moderately) dense active suspensions: the decomposition of water peroxide [41] and the reversible, spinodal demixing of a binary water–lutidine solvent [42].

While aggregation of catalytic swimmers has been observed before [21], clusters of active colloids have been characterized the first time in experiments performed by Theurkauff et al. [24]. They prepared the so-called Janus particles consisting of two surfaces with different physical properties. In this particular experiment they used spherical gold

particles with one hemisphere coated with platinum. Immersing these particles in a solvent containing hydrogen peroxide H_2O_2, the particles are propelled along their symmetry axis. The propulsion is realized due to the different chemical properties of platinum and gold, leading to different rates of H_2O_2 consumption, see Fig. 1(c). The mechanism that is actually responsible for the propulsion (diffusiophoresis, electrophoresis, or a combination of both) is still somewhat debated, see Ref. [43] for a more detailed account for polystyrene-Pt swimmers. At sufficient low concentrations of hydrogen peroxide, the propelling speed is proportional to the H_2O_2 concentration. Of course, at some point, the swimming velocity saturates due to the finite number of active sites on the particle surface [44]. The swimming motion of a single particle, as measured by the mean-squared displacement, fits excellently with the prediction of a simple theoretical model [22,45,46], which is discussed in Section 3.1. The experiment can even be performed at high densities since particles do self-propel at H_2O_2 concentration below 0.1 %, which, in addition, prevents the creation of unfavorable O_2 bubbles.

In order to realize different density regimes, Theurkauff et al. have confined particles in a slightly tilted cell, which creates a reduced gravity field. The resulting sedimentation profile is more stretched compared to the equilibrium case, giving the possibility to study the system at different densities corresponding to different heights in one single sample, see Fig. 1(a). At low to intermediate densities, the suspension shows the formation of several clusters, cf. Fig. 1(b). Once clusters are formed, particles do not stay in their initial cluster but are continuously exchanged between clusters, see Fig. 1(b). For a better understanding of this cluster phase, the structure factor has been measured, which shows that clusters are highly ordered with pronounced peaks at values of the wave vector k corresponding to the hexagonal lattice. Simultaneously, an apparently diverging behavior for $k \to 0$ is observed, which has been the first experimental indication of density

---

[1] Thermophoresis could in principle also work [39,40], but the required high illumination powers induce optical forces, which, in the context considered here, are less desirable.

fluctuations at large length scales for self-propelled beads. This observation is typical for systems exhibiting finite cluster phases, which can also be seen for passive colloids with attractive interactions [47].

Further studies at intermediate densities for packing fractions $\phi = 0.03 - 0.5$ in a nontilted cell show a linear correlation between mean cluster size and the average velocity of the particles. This is corroborated by a theoretical description based on the chemotactic Keller–Segel model [48]. The use of this model is justified through the fact that each particle creates a monopole field of H_2O_2 or O_2 around itself, which acts as chemoattractant for nearby particles. One of the solutions of the model includes a collapse of the structure into dilute and dense regions [49]. Although the model does not provide a description for the kinetics of the clusters, the threshold for this collapse, i.e., the number of particles in a dense region, is shown to be proportional to the particle velocity in agreement with the mean cluster size in the experiments.

In the second experiment, Palacci et al. [25] have performed experiments on catalytic colloidal swimmers, in which the propulsion can be controlled by light. The particles consist of an antiferromagnetic hematite cube enclosed by a polymer sphere in such a way that a part of the hematite cube is exposed to the solvent. When particles are again immersed in a solvent mixture containing H_2O_2 the system is in thermal equilibrium in the case of bright-field illumination. As soon as the suspension is illuminated by the blue-violet light (430 to 490 nm), particles can be described as two-dimensional swimmers. The mechanism behind the propulsion is that the blue-violet light triggers the chemical decomposition of hydrogen peroxide at the exposed part of the hematite cube. In addition the hematite cube instantly points towards the cell walls and propels the particles to the system boundaries. The colloids then surf on the induced osmotic flow and their motion is captured by the model of self-propelled Brownian particles in two dimensions, which will be introduced in Section 3.1. The experiment shows the formation of a few big crystalline clusters just like the interchange of particles between different clusters, see Fig. 1(d).

Furthermore, Palacci et al. show that the system exhibits a transition regarding the number fluctuations $\Delta N \propto N^\alpha$, where the exponent changes from its equilibrium value $\alpha = 1/2$ to giant number fluctuations with exponent $\alpha \approx 0.9$ at $\phi \approx 0.07$. Note that these giant number fluctuations are nothing specific for active systems, since $\alpha = 1$ is expected for any phase separating system. One central result of this experiment

is the reversibility of the cluster phase. Once clusters are formed and the illumination is turned off subsequently, one observes that all clusters dissolve, which shows the absence of equilibrium attractions that are sufficiently strong to induce accumulation of particles. However, the authors report a strong phoretic attractive force when particles are active. This is demonstrated by analyzing the radial velocity v_r between particle pairs showing the relation $v_r \sim r^{-2}$ which is characteristic for phoretic attraction. In order to show that the activity and not the phoretic attraction is responsible for the clustering, one can apply an external magnetic field, causing all particles to propel themselves in the direction of the magnetic field. It is shown that such a directed non-diffusive propulsion is not sufficient to maintain a given cluster, because particles drift apart due to diffusion, i.e., phoretic attraction is not strong enough. As soon as the magnetic field is turned off and illumination is turned on again, the cluster reforms. This demonstrates experimentally that clustering of self-propelled beads is caused by a self-trapping mechanism that essentially depends on the combination of both self-propulsion and rotational noise.

2.2. Phase separation

Buttinoni et al. have used a different experimental setup of colloidal self-propelled Janus particles that are, however, not driven by chemical reactions [23,42,26]. The spherical particles are prepared from silica beads, where one hemisphere is coated with carbon. Here, particles are confined between two glass slides in a quasi-two-dimensional geometry and are suspended in a water-2,6-lutidine mixture, which at room temperature is just below the critical temperature ~33 °C. When the suspension is illuminated by a widened laser beam (532 nm), the carbon absorbs the light and the solvent is locally heated above the critical point. Consequently, the solvent demixes locally at the carbon side of the particles. The particles behave as Brownian self-propelled particles in two dimensions with a propelling speed that is proportional to the light intensity [23,42]. The propulsion mechanism is diffusiophoresis [42]. Carbon has been employed as a light-absorbing material since its Hamaker constant is substantially lower compared to gold (or any other metal). Attractive forces in the passive suspension are thus almost negligible as demonstrated by the measured pair distribution function [26]. Another advantage of this setup compared to catalytic colloidal swimmers is that for the considered light intensities phoretic attraction can also be neglected. While it has been shown that, in principle, there exists a phoretic attraction between particles for sufficient high light intensities, active suspensions have been studied at intensities far below this threshold. This has been tested by measuring the pair distribution function for spherical passive particles in the vicinity of a Janus particle stuck to the glass slide both in and out of equilibrium, whereby no qualitative deviations have been observed.

Again, the experiment of Buttinoni et al. shows the formation of clusters as soon as the particles are activated (see Fig. 2). At low densities, a linear relation between mean cluster size and particle speed v_0 is found similar to the other two experiments in Refs. [24,25]. The clustering mechanism can be described as the competition between two time scales, which has also been done in Refs. [29,50] in terms of a kinetic model. The physical picture is that of colliding particles, which block each other ("self-trapped") due to the persistence of their motion, where orientations decorrelate on time scales $\sim 1/D_r$ with rotational diffusion coefficient D_r. If this rotational diffusion is slow enough compared to the mean free time, other particles may join the cluster before the initial particles are able to escape the "seed", cf. Fig. 2(b). After sufficient time, a dynamic steady state should be reached, where on average just as many particles escape the cluster as new particles join the cluster. Clusters are indeed very dynamic objects, where particles are interchanged continuously, see Fig. 2. Moreover, it has been possible to resolve particle orientations so that the self-trapping mechanism could be confirmed qualitatively, cf. Fig. 2(b). When illumination
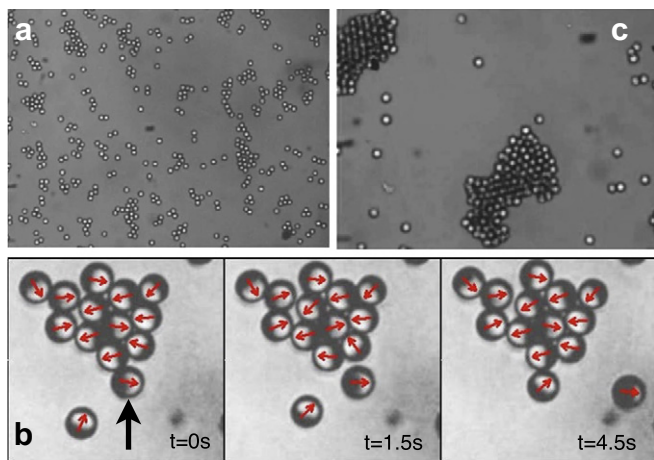

Fig. 2. Carbon-coated colloidal self-propelled particles in a locally demixing water–lutidine mixture: (a) Cluster formation at low densities ($\phi \simeq 0.1$). (b) Resolved particle orientations and observation of particle interchange. If the particle rotational diffusion is fast enough, it escapes an initial cluster before other particles join the cluster. The snapshots show one such event, where a particle (arrow) leaves the cluster and is replaced by another particle. (c) Evidence for phase separation at higher densities.
Figure adapted from Ref. [26].

is turned off, clusters dissolve until the system reaches thermal equilibrium.

At higher densities, the experiment of Buttinoni et al. shows a gas phase with a few big and slowly moving clusters, see Fig. 2(c). Following the passive scenario of phase separation, one might expect the final state to contain one single large cluster. However, larger clusters move very slowly so that the actual merging of all clusters is not observed within the experimental time window. For example, clusters in the experiment are not perfectly two dimensional objects (they might "buckle" out-of-plane) and approaching the cell walls they slow down. Nevertheless, while monitoring a region consisting N particles, all particles in clusters larger than $N/10$ have been added up and the fraction of total particles in a cluster is identified as the order parameter P. By measuring this order parameter for different propelling speeds and densities, one observes a continuous increase, which is moreover supported by Brownian dynamic simulations as discussed in the next section. The transition occurs at lower densities than predicted by the simulations of perfectly hard disks. Still, the critical swimming speeds obtained from experiments and simulations at intermediate packing fraction $\phi = 0.36$ coincide quite well.

Although each experiment shows an individual method to prepare self-propelled particles, we observe dynamical clustering to be quite generic. To gain further insight into the phase behavior, we seek assistance from analytical and numerical work as detailed in the next section.

3. Model and numerical results

3.1. Model

In order to analytically and numerically study suspensions of self-propelled colloidal particles, one needs a suitable minimal model for the experiments discussed in the previous section that is both simple and tractable, but contains the relevant physics. Assuming that the dynamics is overdamped as appropriate for solvated colloidal particles at low Reynolds numbers, the Langevin equation is applicable, i.e.,

$$\dot{\mathbf{r}}_i = -\mu_0 \nabla U + v_0 \mathbf{e}_i + \xi_i. \tag{1}$$

The mobility of a free particle is denoted by μ_0. The noise term ξ_i models the thermal motion and has zero mean and variance

$$<\xi_i(t)\xi_j^T(t')> = 2D_0\mu_0^{-2}\delta_{ij}\delta(t-t'), \tag{2}$$

with $D_0 = k_B T \mu_0$ denoting the bare diffusion coefficient and $k_B T$ the thermal energy. Particles are restricted to two dimensions and interact via a pair potential $u(r)$, where the total energy is given by $U = \sum_{i<j} u(|\mathbf{r}_i - \mathbf{r}_j|)$. Each particle has an orientation $\mathbf{e}_i = (\cos \varphi_i, \sin \varphi_i)$, along which the particle is propelled with a constant speed v_0. Of course, the model does not resolve the microscopic origin of the directed motion but requires v_0 as an input parameter. The orientational angle φ_i fluctuates freely with diffusion coefficient D_r according to

$$<\dot{\varphi}_i> = 0, \quad <\dot{\varphi}_i(t)\dot{\varphi}_j(t')> = 2D_r\delta_{ij}\delta(t-t'). \tag{3}$$

On time scales $\gg 1/D_r$, the motion of a *single* propelled particle becomes effectively diffusive with increased long-time diffusion coefficient $D_{eff} = D_0 + v_0^2/(2D_r)$ [44], making it possible to define an effective temperature $T_{eff} \sim v_0^2$, which is strongly modified for interacting particles [32,51]. In the case of free particles it has been shown that particles being trapped in a harmonic external potential, do not follow the concept of an effective temperature, while the sedimentation of free self-propelled particles is describable in terms of an effective temperature [22,53,52]. In the following, we now review the key results from numerical studies of the particle model based on Eq. (1).

3.2. Freezing

The model just described has been used first by Bialké et al. to study the freezing transition of an active suspension at high densities [51]. Particles interact via the Yukawa pair potential $u(r) = \Gamma e^{-\lambda r}/r$ with a fixed inverse screening length $\lambda = 3.5$ leaving the coupling strength Γ and the free swimming velocity v_0 as free parameters. By applying both static and dynamic criteria for the freezing and melting, it is shown that the suspension is first ordered structurally before dynamical freezing can be observed. As a structural measure the local hexagonal bond-orientational order has been evaluated, which is quantified through

$$q_6(i) = \frac{1}{|\mathcal{N}(i)|} \sum_{j \in \mathcal{N}(i)} e^{i6\theta_{ij}}. \tag{4}$$

Here, θ_{ij} is the angle enclosed between the displacement vector of particles i and j and a fixed axis, and $\mathcal{N}(i)$ is the set of the neighbors of particle i, usually within a threshold distance. By averaging q_6 over all particles and squaring its absolute value, one gets a global structural order parameter which is 0 for an unordered suspension and 1 for a perfect hexagonal crystal. Note that although a large cluster might show a high crystalline order, this global parameter is still 0 due to the particles in the gas phase and the crystalline domains within the cluster which are tilted to one another and separated by linear defects [29]. However, by increasing the propulsion speed, the transition to a hexagonal crystal is shifted towards higher critical coupling strengths $\Gamma_c \sim \sqrt{\phi}/T$. Another result of this work has been that, similar to the clustering transition, the shifted freezing transition cannot be described by an effective temperature $T_{eff} \sim v_0^2$. In related studies, Berthier et al. [54,55] have shown that a glass forming system exhibits a shift towards higher temperatures for the kinetic arrest to occur if particles are active. It appears that this shift cannot be explained by the simple picture of an effective temperature, but allows the study of glasses at high packing fractions [56]. In yet another numerical study for a soft interaction potential of a polydisperse suspension, Fily et al. [32] have resolved the complete phase diagram, where a fluid, a phase separated regime and, due to the polydispersity, a glassy regime is identified, see Fig. 4(b).

3.3. Clustering

By now, extensive numerical simulations of the minimal model have been performed by several groups employing different repulsive pair potentials [26–33]. The clustering and phase separation of athermal self-propelled particles have been reported first by Fily and Marchetti in Ref. [27] employing the minimal model. For particle interactions, the authors have chosen a non-diverging pair potential, i.e., harmonic repulsion in the case of particle overlap. Moreover, the authors neglect translational noise ($D_0 = 0$) and treat rotational diffusion as an independent fixed parameter. They perform molecular dynamics simulations of a monodisperse suspension with up to 10,000 particles. They show that systems above $\phi \approx 0.4$ phase separate into one big cluster surrounded by a gas phase. The experimentally observed clustering at lower densities (Refs. [24,25]) and phase separation into a few big and slow clusters (Ref. [26]) are not observed in the simulations. However, in qualitative agreement with the experiment by Palacci et al. [25], giant number fluctuations have been reported for suspensions above the critical density. Furthermore, the behavior cannot be mapped to a system with an effective temperature $T_{eff} \sim v_0^2$ in agreement with [51]. Finally, in accordance with the experiment by Theurkauff et al. an apparently diverging behavior of the static structure factor for $k \to 0$ is found for phase separated systems.

Even larger systems with up to 512,000 particles have been simulated by Redner et al. [29]. In contrast to the previous work, particles interact through the WCA potential [57] as appropriate for hard colloidal
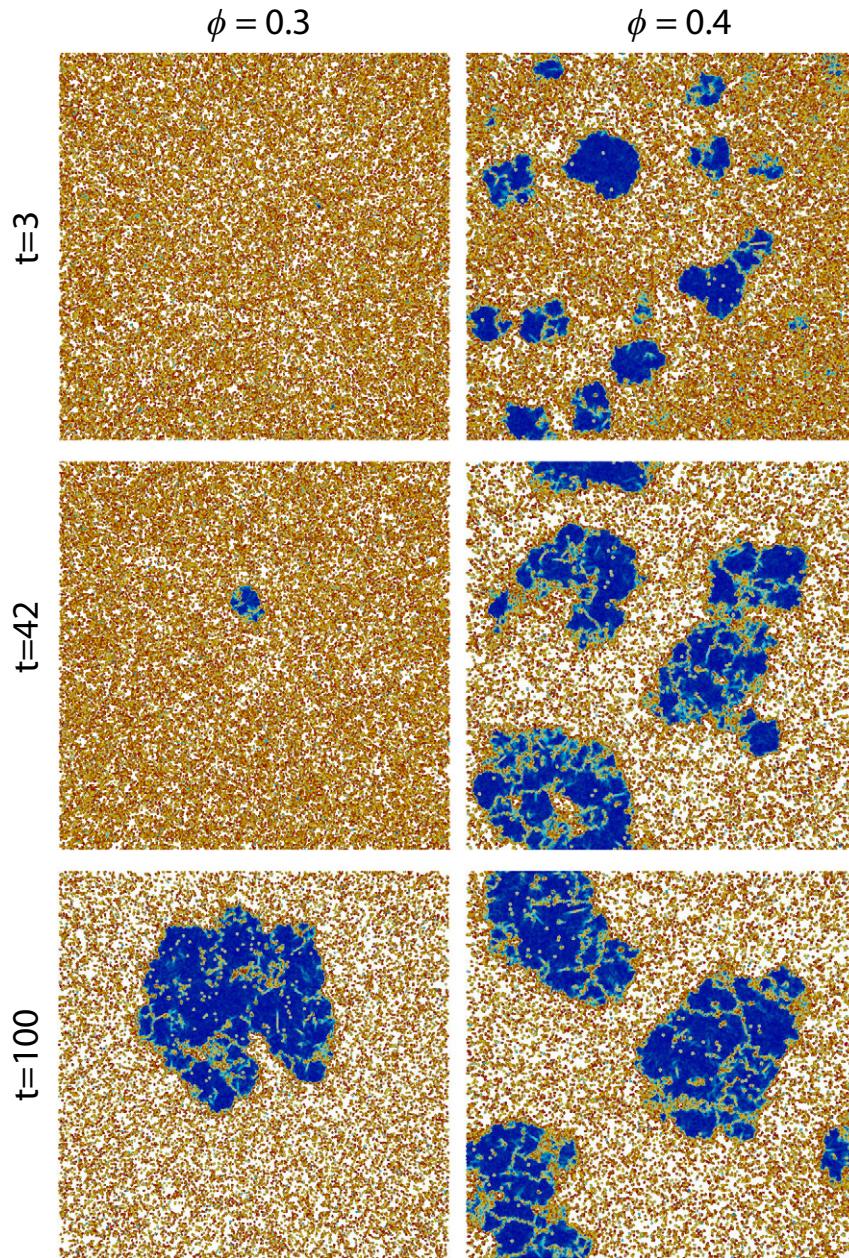
$$\phi = 0.3 \qquad \phi = 0.4$$

Fig. 3. Phase separation dynamics for the minimal model at two densities: area fraction $\phi = 0.3$ (left) and $\phi = 0.4$ (right). The snapshots show particle-resolved simulations for $N = 40000$ particles at three different times given in units of a typical Brownian time. The suspension is equilibrated at $v_0 = 0$ and then quenched instantaneously to $v_0 = 100$. At lower density we observe a nucleation-type scenario: after a delay one single cluster starts to grow until the steady state is reached. In contrast, at higher density multiple domains form immediately after the quench and then grow and merge until eventually a single dense droplet is reached. This scenario is usually described as spinodal decomposition. Particles are colored according to their q_6 value, where red particles correspond to $q_6 = 0$ and blue particles to $q_6 = 1$.

particles. Translational noise is included and the rotational diffusion coefficient is coupled to translational diffusion via the Stokes–Einstein–Debye relation $D_r = 3D_0/a^2$, where a is the particle diameter which is defined through the potential. By varying the packing fraction ϕ and the propulsion speed v_0, extensive simulations have lead to a phase diagram characterized by the fraction of particles in the dense cluster phase. Again, similar to Fily and Marchetti in Ref. [27], a clustering transition is observed. Moreover, a remarkable result is that a simple model of rate equations for particles joining and leaving a given cluster shows excellent agreement with the numerical data. The authors also studied structural properties within the dense phase through bond-orientational order, cf. Eq. (4), where one notices 5-fold and 7-fold

point defects as well as linear defects separating crystalline domains within the cluster. The authors also measure the spatial correlation of the bond-orientational order parameter in large clusters, where they observe a transition from liquid-like exponential decay to a hexatic-like power-law decay as they increase the swimming speed, which is similar to the freezing by heating transition observed by Helbing et al. [58]. Furthermore, different phase separation scenarios are observed: on the one hand the system shows delayed nucleation like an equilibrium system near the binodal and one observes the growth of one single cluster. On the other hand, a denser system shows a spinodal-like coarsening behavior with several clusters (see Fig. 3 for data obtained for a similar system). Redner et al. also report that the asymptotic growth

of the mean cluster size follows $\sim t^{1/2}$. However, the value of the exponent has to be treated with care and more recent results indicate an asymptotic value of 1/3, which is also expected for passive phase-separated suspensions [33,59].

In Fig. 4 two numerical phase diagrams for the minimal model are presented. In Fig. 4(a) results employing the hard WCA potential are shown, where a range of state points (ϕ, v_0) have been simulated. In Fig. 4(b), a similar model has been studied but without translational noise and employing a much softer repulsive potential, that allows particles to overlap. Moreover, the particle sizes are not identical but drawn from a distribution. As mentioned, this leads to a qualitative change at high densities with the appearance of a glassy phase. Together, these results demonstrate that the described phase separation in active suspensions with a purely repulsive pair potential is a robust phenomenon that does not depend so much on the interaction details.

3.4. Hydrodynamic effects

Although the numerical results shown have been obtained using the simple particle model given by Eq. (1), one already observes qualitatively quite good agreement with the experiments. For a more faithful modeling of the experimental setups one needs to include hydrodynamic interactions, not only between particles, but also between particles and confining walls. One promising direction is the hydrodynamic model derived by Ishikawa et al., which prescribes the tangential surface velocity $\mathbf{v}_i^s$ of the fluid at swimmer i according to

$$\mathbf{v}_i^s = B_1 \left(1 + \beta \mathbf{e}_i \cdot \mathbf{r}_i^s \right) \left[(\mathbf{e}_i \cdot \mathbf{r}_i^s) \mathbf{r}_i^s - \mathbf{e}_i \right], \tag{5}$$

where $\mathbf{r}_i^s$ denotes the normalized vector pointing from the particle center to a surface point [60]. This type of hydrodynamic swimmers is called *squirmers*. The free swimming velocity is proportional to B_1, while the factor of proportionality depends on the spatial dimensions of the system. The quantity β determines the symmetry of the velocity field and characterizes a particle with $\beta < 0$ as "pusher" and with $\beta > 0$ as "puller" [61]. For $\beta = 0$, the velocity field at the particle surface is symmetric and the particle can be considered as a neutral squirmer. For the connection between propulsion mechanism and the squirmer model, see, e.g., Ref. [62].

For suspensions of active particles, the required computational power limits the total number of particles that can be simulated to currently a few hundreds so that results have to be analyzed carefully regarding finite size effects. Ishikawa and Pedley [63] have simulated up to 196 squirmers restricted to a two-dimensional motion in a monolayer within in an unbounded three-dimensional fluid. Although particles tend to align, which counters the self-trapping mechanism discussed before, they observe the formation of clusters. In addition they have considered bottom-heavy particles, i.e., particles with a shifted center of mass, which tend to swim upwards and are able to prevent sedimentation [64]. In this case the formation of bands is observable. Another work by Fielding [65] considers 256 neutral squirmers restricted to two dimensions in a two-dimensional fluid. It is shown that phase separation is strongly suppressed due to hydrodynamic interactions. The mechanism responsible for the suppression is an effective hydrodynamic torque turning particle orientations so that head-on collisions (and thus the trapping time) are reduced. More recently, Zöttl and Stark [66] have considered 208 squirmers moving in strong confinement. In the case of $\beta \neq 0$ they also found that phase separation is suppressed. However, neutral squirmer phase separates more clearly into a crystal phase and a gas phase than particles modeled by Eq. (1). This effect is caused by a slow down due to hydrodynamic interaction between particles and hydrodynamic swimmer–wall interactions. The authors show that the angular distribution of the squirmers is broadened and particles also tend to orient perpendicular to the cell wall thus enhancing the self-trapping mechanism. This could be one of the reasons why
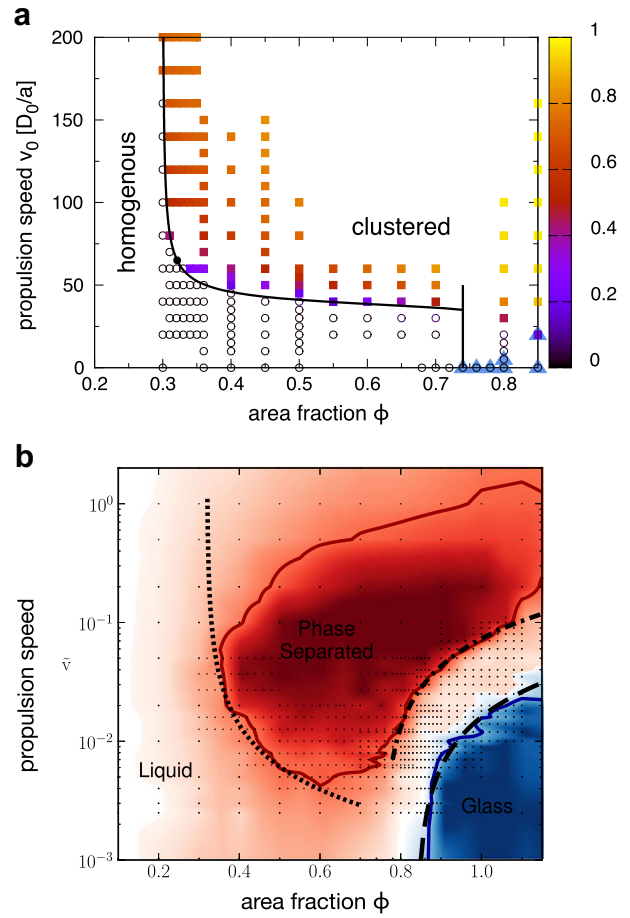

Fig. 4. Numerical phase diagrams: (a) For a monodisperse active suspension in which particles interact via the short-ranged repulsive WCA potential. The color scale corresponds to the fraction of particles in the dense phase, whereby open symbols indicate a homogeneous suspension and closed symbols indicate the clustered phase. Also shown is a prediction for the instability line (solid and dashed lines). The vertical dashed line indicates the equilibrium freezing density with triangles corresponding to the solid state as identified from the bond-orientational order parameter Eq. (4). (b) For a polydisperse active suspension (neglecting translational noise) employing a soft repulsive pair potential. Here a glassy region instead of freezing is observed. Red regions correspond to systems with high number fluctuations, while blue ones show systems with slow dynamics. Adapted from Ref. [33] and arXiv:1309.3714v1.

experimental systems tend to cluster at lower densities than observed in the Brownian dynamics simulations neglecting hydrodynamics.

4. Mean-field theory

4.1. Derivation

We now briefly sketch the systematical derivation of the coupled mean-field, effective hydrodynamics equations of motion developed in Ref. [30]. As a starting point, we note that an equivalent description of the numerical model given by Eq. (1) is provided through the Smoluchowski equation

$$\partial_t \Psi_N = \sum_{i=1}^{N} \nabla_i \cdot \left[(\nabla_i U) - v_0 \mathbf{e}_i + \nabla_i \right] \Psi_N + D_r \sum_{i=1}^{N} \frac{\partial^2 \Psi_N}{\partial \varphi_i^2}, \tag{6}$$

where $\Psi_N(\{\mathbf{r}_i, \varphi_i\}, t)$ is the joint probability distribution of all possible configurations. Since particles are identical, one random particle is tagged and the subscript for position and orientation is dropped. Then,
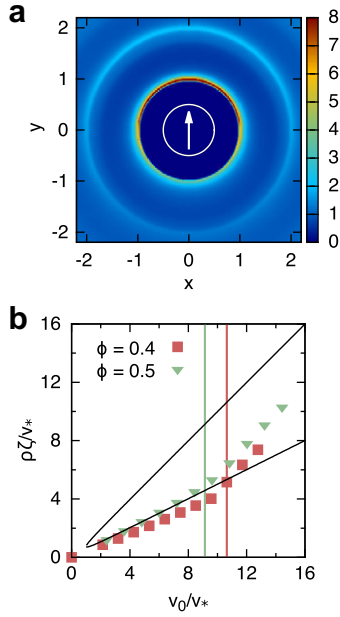
Fig. 5. (a) Anisotropic pair distribution function from numerical simulations using the WCA potential plotted in the xy-plane. The white circle represents the tagged particle with the white arrow indicating the particle orientation. (b) Plot of the normalized force imbalance coefficient $\bar{\rho}\zeta/v_*$ as a function of the reduced swimming speed v_0/v_* for two area fractions ϕ. The characteristic speed is set by $v_* = 4\sqrt{DD_r}$. The dashed vertical lines correspond to the phase transition points determined with the help of finite-size scaling. The two solid lines represent the boundaries of the instability region determined by Eq. (18).
Adapted from Ref. [30].

Ψ_N is integrated over all other particle positions and orientations to obtain the one particle probability distribution $\Psi_1(\mathbf{r},\varphi,t)$. Its evolution obeys

$$\partial_t \Psi_1 = -\nabla \cdot [\mathbf{F} + v_0 \mathbf{e}\Psi_1 - \nabla\Psi_1] + D_r \partial_\varphi^2 \Psi_1, \tag{7}$$

where $\mathbf{F}$ is the mean force acting on the tagged particle, which depends on higher many-body probability distributions and leads to the well-known BBGKY hierarchy [67].

As a closure already on the level of the single particle density, we project the mean force onto the orientation of the tagged particle, $\mathbf{F} \approx (\mathbf{e} \cdot \mathbf{F})\mathbf{e}$ and introduce an effective diffusion coefficient (for details see Ref. [30]). We thus find the mean-field evolution equation for the one particle density.

$$\partial_t \Psi_1 = -\nabla[v(\rho)\mathbf{e} - D\nabla]\Psi_1 + D_r \partial_\varphi^2 \Psi_1. \tag{8}$$

Here, ρ denotes the local density, D the long time diffusion coefficient in a passive suspensions, and

$$v(\rho) = v_0 - \rho\zeta \tag{9}$$

is the effective swimming speed. Here, we have assumed that the local density $\rho(\mathbf{r},t)$ is a sufficiently slowly varying field so that we can replace the homogeneous density $\bar{\rho}$ with the local density $\rho(\mathbf{r},t)$. This assumption holds close to the onset and during the initial stages of the dynamical instability. Although a linearly decaying $v(\rho)$ has been considered before [34], Bialké et al. have shown the derivation from first principles.

The effective swimming speed given by Eq. (9) is reduced due to the interactions with other particles as quantified by the force imbalance coefficient

$$\zeta = \int_0^\infty dr\, r\left[-u'r\right]\int_0^{2\pi} d\theta \cos\theta g(r,\theta), \tag{10}$$

where the prime denotes the derivative with respect to the argument and θ is the angle enclosed between the orientation of the tagged particle and the displacement vector from the tagged particle to another particle at distance r. The physical picture behind Eq. (9) is that particle collisions are more likely occurring in the direction of propulsion, causing an anisotropic two-dimensional pair distribution function $g(r,\theta)$. This picture is confirmed in computer simulations, see Fig. 5(a). While we found a linear relationship Eq. (9), Cates and coworkers have considered more general functional dependences $v(\rho)$ and have shown that a reduced particle mobility in dense regions might lead to further accumulation of particles in these regions and finally to phase separation [36–38]. Note that the competition of time scales is also reflected in Eq. (9). The mean collision rate is connected to the density ρ and swimming speed v_0, while the rate of reorientation influences the value of ζ. This is demonstrated in the limit $D_r \to \infty$, where orientational fluctuations are so fast that on average the pair distribution function is isotropic and the force imbalance vanishes, $\zeta = 0$.

The local density $\rho(\mathbf{r},t)$ and the orientational field $\mathbf{p}(\mathbf{r},t)$ are given by

$$\rho(\mathbf{r},t) = \int_0^{2\pi} d\varphi \psi_1(\mathbf{r},\varphi,t) \tag{11}$$

and the first moment

$$\mathbf{p}(\mathbf{r},t) = \int_0^{2\pi} d\varphi \mathbf{e}\psi_1(\mathbf{r},\varphi,t), \tag{12}$$

respectively. The equations of motion for these two fields become the continuity equation

$$\partial_t \rho = -\nabla \cdot [v\mathbf{p} - D\nabla\rho] \tag{13}$$

for the density and, through neglecting the coupling to second harmonics of the orientational angle,

$$\partial_t \mathbf{p} = -\frac{1}{2}\nabla(v\rho) + D\nabla^2\mathbf{p} - D_r\mathbf{p}. \tag{14}$$

The first term on the right hand side can be interpreted as an effective pressure $P(\rho) = \frac{1}{2}v(\rho)\rho$, the second term is akin to a viscosity term, and the last term describes the local relaxation due to the rotational diffusion. While these equations have been derived systematically from the Smoluchowski Eq. (6), they can also be obtained from the phenomenological equations of Toner and Tu [68] (see, e.g., Ref. [32]) by neglecting all higher order terms. Of course, in this case the various coefficients are in principle unknown.

4.2. Dynamical instability

The linear stability of Eqs. (13) and (14) against density fluctuations has been studied by Speck et al. and Fily et al. [27,30,32,33]. By considering large length scales and time scales much longer than $1/D_r$, Eq. (14) can be written as

$$\mathbf{p} \approx -\frac{1}{2D_r}\nabla(v\rho), \tag{15}$$

so that the orientational field is adiabatically connected to the density field. By putting this expression into Eq. (13), we obtain the diffusion equation

$$\partial_t \rho = \nabla\mathcal{D}(\rho)\nabla\rho. \tag{16}$$

While we have thus eliminated the orientational field **p**, the effects of the force imbalance are retained through the effective swimming speed and give rise to a density-dependent, collective diffusion coefficient.

$$\mathcal{D}(\rho) = D + \frac{(v_0 - \rho\zeta)(v_0 - 2\rho\zeta)}{2D_r} \qquad (17)$$

If $\mathcal{D}(\rho) < 0$ the system becomes locally unstable and density fluctuations grow exponentially until they saturate due to the coupling to nonlinear modes. The criterion $\mathcal{D}(\rho) < 0$ is fulfilled if $\zeta_- \leqslant \zeta \leqslant \zeta_+$ with

$$\frac{\overline{\rho}\zeta_\pm}{v_*} = \frac{3}{4}(v_0/v_*) \pm \frac{1}{4}\sqrt{(v_0/v_*)^2 - 1}. \qquad (18)$$

This result implies that at least a propulsion speed $v_0 > v_* = 4\sqrt{DD_r}$ is necessary for the instability to occur, see Fig. 5(b).

This prediction has been tested for numerical results employing the WCA potential, see Fig. 5(b). For two densities, the transition speeds v_c have been estimated with the help of finite-size scaling of an order parameter, in our case the mean fraction of particles in the largest cluster [30]. For each propulsion speed v_0 we have also determined the force imbalance through Eq. (10) from the measured pair distribution function, and the passive long-time diffusion coefficient D at that density, which determines v_*. The result in Fig. 5(b) shows good agreement between the estimated transition speeds v_c and the crossing of the imbalance coefficient into the instable region.

5. Concluding remarks

To conclude, we have reviewed experimental, numerical, and analytical work on the phase behavior of self-propelled colloidal particles without explicit alignment interactions in (quasi-)two dimensions. Although different physical mechanisms are responsible for the "swimming" of particles in the three experimental setups, clustering of particles is observed to be a generic, robust feature of active suspensions. Supported by computer simulations of a minimal model, it has been established that the self-propulsion of repulsive particles is able to induce a phase separation into dense and dilute regions. In the mean-field picture, this phase separation can be explained as a dynamical instability, where in the dilute regions the fast particles exert an effectively higher pressure compared to dense but slow regions. Although active suspensions are genuinely out-of-equilibrium systems, this phenomenon is surprisingly similar to liquid-vapor phase separation in a passive suspension with sufficiently strong attractive interactions. At higher densities, the self-propulsion shifts the freezing (or glass-forming) transition. In particular, at fixed density the suspension is melted before entering the phase-separated state as the propulsion speed is increased.

The pivotal role in the mean-field theory is played by the force imbalance. This takes into account that the pair distribution function is not isotropic with respect to particle orientations although particles are spherical. In computer simulations, we found good agreement with the mean-field prediction for the onset of the dynamical instability.

Departing from the minimal model, there are several directions into which further studies might go. Recently, first studies have started to investigate the phase behavior of the minimal model in three dimensions [31,69] and the influence of attractive forces [50,70] or non-spherical particle shape [16,71]. Active particles (bacteria or colloidal particles) with entropic attraction due to depletants (polymers) have been studied in Refs. [72,73], showing that phase separation is suppressed if alignment interactions are introduced. For catalytic swimmers, the effects of local fuel depletion leading to collective chemotactic behavior have started to receive attention [74–76].

Another open issue is the more faithful modeling of the experiments in order to achieve more than qualitative agreement. An important step is to include hydrodynamic interactions. While the squirmer model seems to be a good starting point, it is not yet clear to which extent it reproduces the actual flow pattern of self-propelled colloidal particles in particular in dense suspensions. Moreover, accessible system sizes are still rather small. From the experimental side, it would be highly desirable to clarify to what degree the propulsion of a particle within a (quasi-two-dimensional) cluster is comparable to free propulsion. This might seem questionable for both the chemically driven particles consuming H_2O_2 as well as the particles driven by reversible demixing of the solvent. In the first case H_2O_2 might be depleted while for the second case shared demixing zones within clusters develop, leading to a reduction of directed motion.

But even for the minimal model Eq. (1) there is plenty of work left to do. For phase transitions in passive systems an elaborate framework has been developed over the years, which allows to reliably construct phase diagrams and to study critical phenomena in finite-size computer simulations. Not much is known yet for active suspensions.

References

[1] T. Vicsek, A. Zafeiris, Phys. Rep. (2012) 71–140 (ISSN 0370-1573).
[2] M.C. Marchetti, J.F. Joanny, S. Ramaswamy, T.B. Liverpool, J. Prost, M. Rao, R.A. Simha, Rev. Mod. Phys. 85 (2013) 1143.
[3] I. Aranson, C. R. Phys. 14 (2013) 518 (ISSN 1631-0705, living fluids/Fluides vivants).
[4] M.C. Marchetti, J.-F. Joanny, S.Ramaswamy, T.B. Liverpool, J.Prost, M.Rao, and R.Aditi simha, ArXiv e-prints (2012), 1207.2929.
[5] A. Cavagna, A. Cimarelli, I. Giardina, G. Parisi, R. Santagati, F. Stefanini, M. Viale, Proc. Natl. Acad. Sci. 107 (2010) 11865.
[6] C. Becco, N. Vandewalle, J. Delcourt, P. Poncin, Phys. A Stat. Mech. Appl. 367 (2006) 487 (ISSN 0378-4371).
[7] F. Peruani, J. Starruß, V. Jakovljevic, L. Søgaard-Andersen, A. Deutsch, M. Bär, Phys. Rev. Lett. 108 (2012) 098102.
[8] H.P. Zhang, A. Beer, E.-L. Florin, H.L. Swinney, Proc. Natl. Acad. Sci. 107 (2010) 13626.
[9] T. Vicsek, A. Czirók, E. Ben-Jacob, I. Cohen, O. Shochet, Phys. Rev. Lett. 75 (1995) 1226.
[10] P. Romanczuk, U. Erdmann, H. Engel, L. Schimansky-Geier, Eur. Phys. J. Spec. Top. 157 (2008) 61 (ISSN 1951-6355).
[11] J. Toner, Y. Tu, Phys. Rev. E. 58 (1998) 4828.
[12] E. Bertin, M. Droz, G. Grégoire, Phys. Rev. E. 74 (2006) 022101.
[13] Y.-L. Chou, R. Wolfe, T. Ihle, Phys. Rev. E. 86 (2012) 021120.
[14] F. Thüroff, C.A. Weber, E. Frey, Phys. Rev. Lett. 111 (2013) 190601.
[15] H.H. Wensink, J. Dunkel, S. Heidenreich, K. Drescher, R.E. Goldstein, H. Löwen, J.M. Yeomans, Proc. Natl. Acad. Sci. 109 (2012) 14308.
[16] H.H. Wensink, H. Löwen, J. Phys. Condens. Matter 24 (2012) 464130.
[17] F.D.C. Farrell, M.C. Marchetti, D. Marenduzzo, J. Tailleur, Phys. Rev. Lett. 108 (2012) 248101.
[18] V. Narayan, S. Ramaswamy, N. Menon, Science 317 (2007) 105.
[19] J. Deseigne, O. Dauchot, H. Chaté, Phys. Rev. Lett. 105 (2010) 098001.
[20] W.F. Paxton, P.T. Baker, T.R. Kline, Y. Wang, T.E. Mallouk, A. Sen, J. Am. Chem. Soc. 128 (2006) 14881.
[21] Y. Hong, N.M.K. Blackman, N.D. Kopp, A. Sen, D. Velegol, Phys. Rev. Lett. 99 (2007) 178103.
[22] J. Palacci, C. Cottin-Bizonne, C. Ybert, L. Bocquet, Phys. Rev. Lett. 105 (2010) 088304.
[23] G. Volpe, I. Buttinoni, D. Vogt, H.-J. Kummerer, C. Bechinger, Soft Matter 7 (2011) 8810.
[24] I. Theurkauff, C. Cottin-Bizonne, J. Palacci, C. Ybert, L. Bocquet, Phys. Rev. Lett. 108 (2012) 268303.
[25] J. Palacci, S. Sacanna, A.P. Steinberg, D.J. Pine, P.M. Chaikin, Science 339 (2013) 936.
[26] I. Buttinoni, J. Bialké, F. Kümmel, H. Löwen, C. Bechinger, T. Speck, Phys. Rev. Lett. 110 (2013) 238301.
[27] Y. Fily, M.C. Marchetti, Phys. Rev. Lett. 108 (2012) 235702.
[28] J. Stenhammar, A. Tiribocchi, R.J. Allen, D. Marenduzzo, M.E. Cates, Phys. Rev. Lett. 111 (2013) 145702.
[29] G.S. Redner, M.F. Hagan, A. Baskaran, Phys. Rev. Lett. 110 (2013) 055701.
[30] J. Bialké, H. Löwen, T. Speck, EPL (Europhys. Lett.) 103 (2013) 30008.
[31] J. Stenhammar, D. Marenduzzo, R.J. Allen, M.E. Cates, Soft Matter 10 (2014) 1489.
[32] Y. Fily, S. Henkes, M.C. Marchetti, Soft Matter 10 (2014) 2132.
[33] T. Speck, J. Bialké, A.M. Menzel, H. Löwen, Phys. Rev. Lett. 112 (2014) 218304.
[34] A. Thompson, J. Tailleur, M. Cates, R. Blythe, J. Stat. Mech. 2011 (2011) P02029 (ISSN 1742-5468).
[35] R. Soto, R. Golestanian, Phys. Rev. E. 89 (2014) 012706.
[36] J. Tailleur, M.E. Cates, Phys. Rev. Lett. 100 (2008) 218103.

[37] M.E. Cates, D. Marenduzzo, I. Pagonabarraga, J. Tailleur, Proc. Natl. Acad. Sci. 107 (2010) 11715.
[38] M.E. Cates, J. Tailleur, EPL (Europhys. Lett.) 101 (2013) 20010.
[39] H.-R. Jiang, N. Yoshinaga, M. Sano, Phys. Rev. Lett. 105 (2010) 268302.
[40] R. Golestanian, Phys. Rev. Lett. 108 (2012) 038303.
[41] W.F. Paxton, K.C. Kistler, C.C. Olmeda, A. Sen, S.K. St.ngelo, Y. Cao, T.E. Mallouk, P.E. Lammert, V.H. Crespi, J. Am. Chem. Soc. 126 (2004) 13424.
[42] I. Buttinoni, G. Volpe, F. Kümmel, G. Volpe, C. Bechinger, J. Phys. Condens. Matter 24 (2012) 284129.
[43] A. Brown, W. Poon, Soft Matter 10 (2014) 4016.
[44] J.R. Howse, R.A.L. Jones, A.J. Ryan, T. Gough, R. Vafabakhsh, R. Golestanian, Phys. Rev. Lett. 99 (2007) 048102.
[45] S.J. Ebbens, J.R. Howse, Soft Matter 6 (2010) 726.
[46] H. Ke, S. Ye, R.L. Carroll, K. Showalter, J. Phys. Chem. A 114 (2010) 5462.
[47] M.E. Cates, M. Fuchs, K. Kroy, W.C.K. Poon, A.M. Puertas, J. Phys. Condens. Matter 16 (2004) S4861.
[48] E.F. Keller, L.A. Segel, J. Theor. Biol. 26 (1970) 399 (ISSN 0022-5193).
[49] M.P. Brenner, L.S. Levitov, E.O. Budrene, Biophys. J. 74 (1998) 1677 ISSN 0006-3495.
[50] G.S. Redner, A. Baskaran, M.F. Hagan, Phys. Rev. E. 88 (2013) 012305.
[51] J. Bialké, T. Speck, H. Löwen, Phys. Rev. Lett. 108 (2012) 168301.
[52] G.Szamel, ArXiv e-prints (2014), 1404.0765.
[53] J. Tailleur, M.E. Cates, EPL (Europhys. Lett.) 86 (2009) 60002.
[54] L.Berthier, ArXiv e-prints (2013), 1307.0704.
[55] L. Berthier, J. Kurchan, Nat. Phys. 9 (2013) 310 (ISSN 1745-2473).
[56] R. Ni, M.A.C. Stuart, M. Dijkstra, Nat. Commun. 4 (2013) 2704.
[57] J.D. Weeks, D. Chandler, H.C. Andersen, J. Chem. Phys. 54 (1971) 5237.
[58] D. Helbing, I.J. Farkas, T. Vicsek, Phys. Rev. Lett. 84 (2000) 1240.
[59] R. Wittkowski, A. Tiribocchi, J. Stenhammar, R.J. Allen, D. Marenduzzo, M.E. Cates, Nat. Commun. 5 (2014).
[60] T. Ishikawa, M.P. Simmonds, T.J. Pedley, J. Fluid Mech. 568 (2006) 119 (ISSN 1469-7645).
[61] J.R. Blake, J. Fluid Mech. 46 (1971) 199 (ISSN 1469-7645).
[62] M.Yang, A.Wysocki, and M.Ripoll, ArXiv e-prints (2014), 1403.0683.
[63] T. Ishikawa, T.J. Pedley, Phys. Rev. Lett. 100 (2008) 088103.
[64] K. Wolff, A.M. Hahn, H. Stark, Eur. Phys. J. E 36 (2013) 1 (ISSN 1292-8941).
[65] S. Fielding, ArXiv e-prints (2012), 1210.5464.
[66] A. Zöttl, H. Stark, Phys. Rev. Lett. 112 (2014) 118101.
[67] J. Hansen, I. McDonald, Theory of Simple Liquids, 3rd ed. Elsevier Science, 2006, ISBN 9780080455075.
[68] J. Toner, Y. Tu, Phys. Rev. Lett. 75 (1995) 4326.
[69] A. Wysocki, R. Winkler, G. Gompper, EPL 105 (2014) 48004.
[70] B. Mognetti, A. Šarić, S. Angioletti-Uberti, A. Cacciuto, C. Valeriani, D. Frenkel, Phys. Rev. Lett. 111 (2013) 245702.
[71] H. Wensink, H. Löwen, Phys. Rev. E. 78 (2008) 031409.
[72] J. Schwarz-Linek, C. Valeriani, A. Cacciuto, M. Cates, D. Marenduzzo, A. Morozov, W. Poon, Proc. Natl. Acad. Sci. U. S. A. 109 (2012) 4052.
[73] S. Das, S. Egorov, B. Trefz, P. Virnau, K. Binder, Phys. Rev. Lett. 112 (2014) 198301.
[74] M. Meyer, L. Schimansky-Geier, P. Romanczuk, Phys. Rev. E. 89 (2014) 022711.
[75] O. Pohl, H. Stark, Phys. Rev. Lett. 112 (2014) 238303.
[76] R. Soto, R. Golestanian, Phys. Rev. Lett. 112 (2014) 068301.